



HAL
open science

Reactive Multiphase Flow in Porous Media at the Darcy Scale: a Benchmark proposal

Stephan de Hoop, Denis Voskov, Etienne Ahusborde, Brahim Amaziane,
Michel Kern

► **To cite this version:**

Stephan de Hoop, Denis Voskov, Etienne Ahusborde, Brahim Amaziane, Michel Kern. Reactive Multiphase Flow in Porous Media at the Darcy Scale: a Benchmark proposal. 2022. hal-03635080

HAL Id: hal-03635080

<https://hal.inria.fr/hal-03635080>

Preprint submitted on 8 Apr 2022

HAL is a multi-disciplinary open access archive for the deposit and dissemination of scientific research documents, whether they are published or not. The documents may come from teaching and research institutions in France or abroad, or from public or private research centers.

L'archive ouverte pluridisciplinaire **HAL**, est destinée au dépôt et à la diffusion de documents scientifiques de niveau recherche, publiés ou non, émanant des établissements d'enseignement et de recherche français ou étrangers, des laboratoires publics ou privés.

Reactive Multiphase Flow in Porous Media at the Darcy Scale: a Benchmark proposal

S. de Hoop¹ D. Voskov^{1,2} E. Ahusborde³ B. Amaziane³ M. Kern⁴

April 8, 2022

1 Introduction and context of the proposal

This document presents a proposal for a benchmark on reactive multiphase flow. The proposal was put together as a followup of the first SITRAM meeting <https://sitram19.sciencesconf.org/>, which took place in Pau in December 2019. The topic is increasingly important for modern energy applications.

The content of the benchmark was initially written by SdH and DV, and the current version is the result of discussions between the five authors. The proposal is still work in progress. Preliminary results were reported by several teams in two sessions of a minisymposium at the upcoming SIAM Conference on Mathematical and Computational Issues in the Geosciences, and it is the organizers' hope that input from the participants will enable the model to be extended towards more realistic geometries as well as physical and chemical phenomena.

A second workshop SITRAM21 <https://sitram21.sciencesconf.org/> was organized in December 2022 at the Inria Center in Paris, where participants showed further results. A special issue of the journal "Computational Geosciences" is planned, where participants will be able to present and compare their work.

The proposal was written to address several challenges commonly met in applications:

1. Robust coupling of chemical reactions with multiphase flow in porous media,
2. Phase behaviour coupling with equilibrium reactions,
3. Conservative treatment of solid phase dissolution and precipitation,
4. Effective coupling of equations in the case of multiple (concurrent) reactions.

The general structure of the physical and chemical model is described in Sections 2 to 5, while the specific data for the proposed cases are given in Section 6, and requested output is specified in Section 7.

2 Governing equations

This section briefly covers the governing equations of the multiphase multi-component reactive transport framework for the proposed benchmark study. We start with the basic mass balance equations including the

¹Delft University of Technology, Delft, Netherlands. S.deHoop-1@tudelft.nl, D.V.Voskov@tudelft.nl

²Stanford University, Stanford, CA, USA

³Universite de Pau et des Pays de l'Adour, E2S UPPA, CNRS, LMAP, Pau, France. etienne.ahusborde@univ-pau.fr, brahim.amaziane@univ-pau.fr

⁴Inria, Paris, France, & CERMICS, ENPC, Marne-la-Vallée, France. michel.kern@inria.fr

effect of chemical reactions as source/sink term following [Kala and Voskov, 2020]:

$$\frac{\partial n_c}{\partial t} + l_c + q_c = \sum_{k=1}^K v_{ck} r_k^K + \sum_{q=1}^Q v_{cq} r_q^Q, \quad c = 1, \dots, C + M, \quad (1)$$

where C is the number of fluid species and M is the number of mineral species, n_c is the overall mass of component c , l_c is the total flux associated with that component, q_c is the total well flow rate associated with that component, v_{ck} is the stoichiometric coefficient associated with kinetic reaction k for the component c and v_{cq} is the stoichiometric coefficient associated with equilibrium reaction q for component c , r_k^K is the rate for kinetic reaction and r_q^Q is the equilibrium reaction rate.

The overall mass of components is defined as

$$n_c = \phi^T \sum_{j=1}^P (\rho_j s_j x_{cj}), \quad c = 1, \dots, C. \quad (2)$$

Here P stands for the total number of fluid phases and x_{cj} is the molar fraction of component c in phase j . This term indicates the total mass of component c in all the fluid phases. For the solid mineral components, we use the following relationship :

$$n_m = \phi^T \rho_m \hat{s}_m, \quad m = C + 1, \dots, M, \quad (3)$$

where \hat{s}_m is the mineral (solid) saturation. The total porosity ϕ^T term will be explained later (see equation 15).

The term l_c defines the flux of component c and is given as:

$$l_c = \nabla \cdot \sum_{j=1}^P (\rho_j x_{cj} \mathbf{u}_j - \rho_j \phi s_j d_{cj} \nabla x_{cj}), \quad c = 1, \dots, C, \quad (4)$$

where the term d_{cj} corresponds to the dispersion of component c in phase j . The term \mathbf{u}_j is the velocity of the phase j and is defined by Darcy's law:

$$\mathbf{u}_j = -k \frac{k_{rj}}{\mu_j} (\nabla p - \rho_j g \nabla h) \quad j = 1, \dots, P, \quad (5)$$

where k is the rock permeability. In this benchmark capillary pressure effects are ignored, so there is only a single pressure for all phases. Equation 1 can be written in a vector form:

$$\frac{\partial \mathbf{n}}{\partial t} + \mathbf{l} + \mathbf{q} = \mathbf{V}^{\mathbf{Q}} \mathbf{r}^{\mathbf{Q}} + \mathbf{V}^{\mathbf{K}} \mathbf{r}^{\mathbf{K}}, \quad (6)$$

where $\mathbf{n} = (n_1, \dots, n_{C+M})^T$, $\mathbf{l} = (l_1, \dots, l_C, 0, \dots, 0)^T$, $\mathbf{q} = (q_1, \dots, q_{C+M})^T$ is the well flow rate, $\mathbf{V}^{\mathbf{Q}}$ and $\mathbf{V}^{\mathbf{K}}$ are the stoichiometric matrices respectively for the equilibrium and kinetic reactions, while $\mathbf{r}^{\mathbf{Q}} = (r_1^Q, \dots, r_C^Q)^T$ and $\mathbf{r}^{\mathbf{K}} = (r_1^K, \dots, r_K^K)^T$ are the equilibrium and kinetic reaction rate vectors.

3 Phase behavior of compositional system

The following equations are used for thermodynamic equilibrium of multicomponent system. A component is in thermodynamic equilibrium if the chemical potentials of the components in both phases are equal:

$$f_{c1} - f_{cj} = 0, \quad c = 1, \dots, C, \quad j = 2, \dots, P. \quad (7)$$

The fugacity of a component in a particular phase is given by

$$f_{cj} = \phi_{cj} x_{cj} p, \quad c = 1, \dots, C, \quad j = 1, \dots, P, \quad (8)$$

where ϕ_{cj} is the fugacity coefficient of an ideal mixture. Equation (7) can also be written in terms of the partition coefficients $K_{cj} = \phi_{cj}/\phi_{c1}$:

$$K_{cj} x_{c,1} - x_{cj} = 0, \quad c = 1, \dots, C, \quad j = 2, \dots, P. \quad (9)$$

The system of equations (7) or (9) can be directly coupled with the conservation equations (6) and solved in a fully coupled manner using the global Newton solver. Such formulation is often called global or natural formulation. However, when a new phase appears in the process of simulation, the phase equilibrium should be calculated based on the local approximation of the mass from equation (6).

The system of equations can be closed with the following algebraic constraints:

$$\sum_{p=1}^P s_p = 1, \quad (10)$$

and

$$\sum_{c=1}^C x_{cj} = 1, \quad j = 1, \dots, P \quad (11)$$

In case of equilibrium reactions, we need to add the law of mass action to either global or local systems (depending on the preferred nonlinear formulation), which is given as:

$$Q_q - K_q = \prod_{c=1}^C a_{cw}^{v_{cq}} - K_q = 0, \quad q = 1, \dots, Q. \quad (12)$$

Here Q is the number of equilibrium reactions, Q_q is the reaction quotient whereas K_q is the equilibrium reaction quotient or equilibrium solubility limit in case of dissolution/precipitation of minerals, a_{cw} is the activity of the component c in the aqueous phase, and v_{cq} is the reaction stoichiometric coefficient.

4 Porosity treatment

For an accurate treatment of solid phase dissolution and precipitation at the continuous level, the treatment of the rock porosity should be adjusted. Conventionally the control volume (denoted as bulk volume) is subdivided into two regions, void space (occupied by all mobile phases, such as liquid and vapor phase) and solid skeleton (occupied by immobile species, for example, carbonate rock).

In most contributions from the literature, the porosity ϕ depends on the concentrations of the minerals according to the relationship:

$$\phi = 1 - \sum_{m=1}^M \frac{\mathcal{M}_m c_{ms}}{\rho_m} = 1 - \sum_{m=1}^M \hat{s}_m, \quad (13)$$

where M is the number of reactive minerals, \mathcal{M}_m is the molar mass of mineral m , ρ_m is the mass density of mineral m and c_{ms} represents the molar concentration of mineral m . Here we introduced saturation of the mineral (solid) phase \hat{s}_m .

In equation (13), it is not clear which properties are spatially correlated and which are changing in time due to dissolution or precipitation reactions. Following the approach suggested in [Farshidi, 2016], we can subdivide the volume of the solid skeleton further into a reactive part which can be modified by chemical

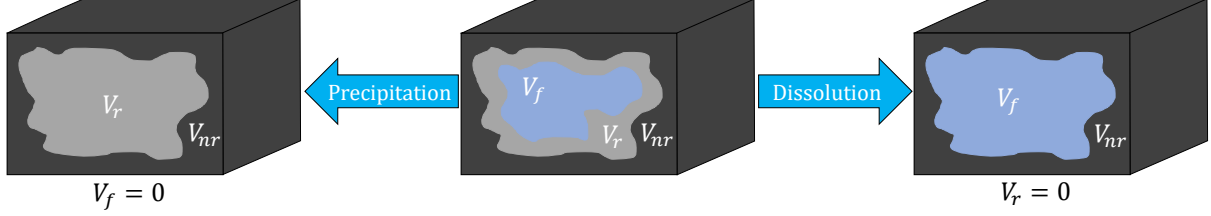


Figure 1: Schematic of the different volumes in the domain. The domain consists of three distinct regions, particularly the fluid volume which is occupied by all the mobile phases (liquid and gaseous in the case of two phase flow), the reactive volume which consists of solid phases that can react or precipitate, and finally the nonreactive volume (the part of the control volume which doesn't participate in any chemical reaction).

reactions and a non-reactive part (which is unaltered by any chemical reaction, and therefore constant throughout the simulation), see Figure 1.

Mathematically this is expressed as follows

$$V_b = V_f + V_r + V_{nr}, \quad (14)$$

where V_r denotes the reactive volume and V_{nr} represents the non-reactive volume (not altered by any chemical reaction). Dividing this by the total (bulk) volume gives

$$1 = \phi + \phi_r + \phi_{nr} = \phi^T + \phi_{nr}, \quad (15)$$

where ϕ_r represents the reactive volume fraction, ϕ_{nr} is the non-reactive volume fraction, and ϕ^T is the total porosity defined as the sum of the fluid porosity and reactive volume fraction. Since only the reactive volume and fluid porosity can change due to chemical reactions, it follows directly that the total porosity remains constant throughout the simulation (when compressibility is neglected). This and the changes in volume fractions due to precipitation and dissolution is illustrated in Figure 1.

Note that the fluid porosity can always be obtained from the following constitutive equation

$$\phi = \phi^T \left(1 - \sum_{m=1}^M \hat{s}_m \right), \quad (16)$$

where M is the number of solid phases (occupying the reactive volume fraction) and \hat{s}_m is the saturation of the solid phase. Please note that the s_α is the fluid saturation (defined over the pore volume) while \hat{s}_m is the solid saturation of mineral phase m (defined over the pore and reactive rock volume).

Solid saturation in the total porosity formulation can be found with the following equation

$$\hat{s}_m = \frac{V_{r,m}}{V_r + V_f}, \quad (17)$$

where $V_{r,m}$ is the volume of mineral phase m defined as

$$V_{r,m} = \frac{\mathcal{M}_m}{\rho_m} n_m^r, \quad (18)$$

where n_m^r is the total number of moles of mineral m that can participate in any reaction.

The permeability dependence on porosity is approximated using the following power-law equation

$$k = k_0 \left(\frac{\phi}{\phi_0} \right)^A. \quad (19)$$

where k_0 and ϕ_0 are initial porosity and permeability respectively.

5 Additional description for fluid and rock parameters

The relative permeability functions used in this benchmark consist of the Brooks-Corey description, more precisely

$$k_{r,\alpha} = k_{r,\alpha}^e \left(\frac{s_\alpha - s_{r,\alpha}}{1 - \sum_{p \in P} s_{r,p}} \right)^{n_\alpha}, \quad (20)$$

where $k_{r,\alpha}$ is the relative permeability, $k_{r,\alpha}^e$ is the maximum relative permeability, $s_{r,\alpha}$ is the residual saturation, and n_α is the Corey exponent of phase α respectively. In the absence of any residual saturation and taking $P = \{w, g\}$ (i.e., assuming liquid (water) and vapor (gas) are the fluid phases present in the system), this results in

$$k_{rw} = k_{rw}^e (s_w)^{n_w}, \quad (21)$$

for the water and

$$k_{rg} = k_{rg}^e (1 - s_w)^{n_g}, \quad (22)$$

for the gas relative permeability.

For the phase density, a simple linear compressibility model is assumed, particularly

$$\rho_\alpha = \rho_{\alpha,0} (1 + C_\alpha (p - p_0)). \quad (23)$$

Here C_α is compressibility and $\rho_{\alpha,0}$ is density at pressure p_0 . This is assumed to hold for each of the three phases present in the system, water, gas, and solid. Additional physical complexity can be obtained by adopting a fully compressible model for the gas phase.

Table 1 describes how each component distributes over all phases.

Component	Liquid (water)	Vapor (gas)	Solid
H ₂ O	✓	✓	✗
CO ₂	✓	✓	✗
Ca ⁺²	✓	✗	✗
CO ₃ ⁻²	✓	✗	✗
CaCO ₃	✗	✗	✓

Table 1: Component-Phase distribution matrix.

Finally, the activity of each component in the water phase can be written using the following equation

$$a_{cw} = \gamma_{cw} m_{cw}, \quad (24)$$

where γ_{cw} is the activity coefficient and m_{cw} is the molality of component c in the water phase, which in turn can be written as

$$m_{cw} = M_w \left(\frac{x_{cw}}{x_{ww}} \right), \quad (25)$$

where M_w is the number of moles of H₂O per kilogram of aqueous phase (typically taken as 55.508), x_{cw} is the mole fraction of component c and x_{ww} is the mole fraction of H₂O in the aqueous phase respectively. For this benchmark the assumption of an ideal solution is made and hence the activity coefficient is taken as 1.

6 Benchmark scenarios

6.1 1D homogeneous domain

The first case is a basic 1D model. The rock and fluid properties are shown in Table 2.

Property	Value	Units
Permeability, $k_{x,y,z}$	[100, 100, 100]	[mD]
Total porosity, ϕ^T	1	[-]
Porosity, ϕ	0.3	[-]
Control volume dimension, $\Delta x, y, z$	[1, 1, 1]	[m]
Number of control volumes, N_x	1000	[-]
Phase density at p_0 , $\rho_{w,g,s}$	[1000, 100, 2000]	[kg/m ³]
Phase compressibility, $C_{w,g,s}$	[10 ⁻⁶ , 10 ⁻⁴ , 10 ⁻⁷]	[1/bar]
Phase viscosity, $\mu_{w,g}$	[1, 0.1]	[cP]
End-point relative permeability, $k_{rw,rg}^e$	[1, 1]	[-]
Corey exponents, $n_{w,g}$	[2, 2]	[-]
Residual saturation, $s_{rw,rg}$	[0, 0]	[-]
Phase partition coefficients, K_{H_2O,CO_2}	[0.1, 10]	[-]
Diffusion coefficients, $d_{cj} = d$	10 ⁻⁹	[m ² /s]
Activity coefficients, $\gamma_{cw} = \gamma$	1	[-]
Porosity-permeability dependence factor, A	3	[-]

Table 2: Values for all the relevant fluid and rock properties.

The model is setup with an injection well (i.e., source term) in the first block and a production well in the last block, no flow boundary conditions from left and right (i.e., $\frac{\partial p}{\partial x}|_{x=0} = 0$ and $\frac{\partial p}{\partial x}|_{x=\Delta x N_x} = 0$). These are typical boundary conditions for reservoir simulation. It is possible to replace the wells and no-flow boundary condition with a Neumann boundary condition at $x = 0$ and a Dirichlet at $x = \Delta x N_x$. Table 3 summarizes the initial, injection and production conditions and simulation time.

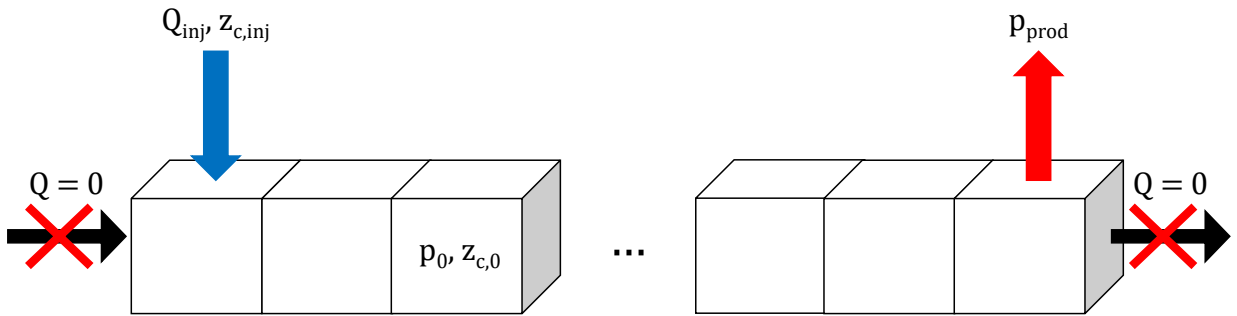


Figure 2: One dimensional domain setup. Injection on the left is constrained with rate and composition Q_{inj} and $z_{c,inj}$ respectively. Production on the right is constrained with pressure p_{prod} . Initial condition for pressure and composition is defined as p_0 and $z_{c,0}$ respectively. No flow boundary condition is imposed on both the left and right boundary.

Property	Value	Units
Injection rate, Q_{inj}	0.2	[m ³ /day]
Injection composition, $z_{c,\text{inj}}, c = 1, \dots, C - 1,$	[0, 1, 0, 0]	[-]
Initial pressure, P_{ini}	95	[bar]
Initial composition, $z_{c,\text{ini}}, c = 1, \dots, C - 1,$	[0.15, 0, 0.075, 0.075]	[-]
Production pressure, P_{prod}	95	[bar]
Simulation time, T	1000	[day]

Table 3: Boundary conditions and other simulation parameters.

Note that the injection and initial compositions are given in terms of the overall mole fractions $z_i, i = 1, \dots, C,$ defined as

$$z_i = \sum_{j=1}^P x_{ij} \nu_j, \quad i = 1, \dots, C,$$

with

$$\nu_j = \frac{\rho_j S_j}{\sum_{k=1}^P \rho_k S_k}, \quad j = 1, \dots, P.$$

We refer to [Kala and Voskov, 2020] for more details. Note that composition for the C -th component can be obtained by $z_C = 1 - \sum_{j=1}^{C-1} z_j$ and is not a primary unknown (hence the initial and injection composition doesn't contain the composition of z_C), and the primary unknowns in this system are $X = [p, z_1, \dots, z_{C-1}]$. The initial and injection composition expressed in terms of molar fraction of individual species and saturation of each phases are given in Appendix A.

We now describe the chemical reaction used for this first case. It consists of a single chemical reaction (i.e., we cannot reduce the global system of nonlinear equation using the element reduction). The system consists of the following components: $z_c = [\text{H}_2\text{O}, \text{CO}_2, \text{Ca}^{+2}, \text{CO}_3^{-2}, \text{CaCO}_3]$. The kinetic reaction equation consists of



We distinguish two cases according to whether the reaction is modelled as kinetic or at equilibrium.

6.1.1 Two-phase flow with kinetic chemistry

Here we assume that the chemical reaction (26) is kinetic. The kinetic rate (i.e., the right-hand-side of equation (6)) is written as

$$r_k = AK_k \left(1 - \frac{Q}{K_{sp}} \right) \quad (27)$$

where A is the reactive surface area, which is a linear function of the solid saturation ($A = A_0 \hat{s}_s = (1 - \phi_0) \hat{s}_s$), K_k is the kinetic reaction constant, Q is the activity product (to simplify $Q = x_{ca,w} \times x_{co3,w}$) and K_{sp} is the equilibrium constant.

The values of the reaction constants are given in Table 4. K_{sp} is equal to $0.25 \times 0.25 = 0.0625$ to ensure that the initial state is in equilibrium and no dissolution occurs.

Property	Value	Units
Kinetic constant, K_k	1	[kmol / m ³ / day]
Solubility constant, K_{sp}	0.0625	[-]

Table 4: Kinetic and equilibrium constants.

6.1.2 Two-phase flow with equilibrium chemistry

The second test case is similar to the first one, except that now the reaction is treated as an equilibrium reaction. Mathematically, this adds an additional constraint equation of the form

$$Q - K_{sp} = 0, \quad (28)$$

where Q is the activity product of the equilibrium reaction as defined in equation (12) (which is taken here to have the same form as in Section 6.1.1) and K_{sp} is the solubility constant, with the value given in Table 3. All the other parameters, fluid/rock/boundary condition/simulation parameters (as specified in table 2 and 3), are the same as for the previous case (including of course the stoichiometry of the reaction).

6.2 2D Heterogeneous domain

The third test case consists of a two-dimensional heterogeneous domain. In the model, a zone of high porosity (and permeability) is embedded within a lower porosity (and permeability) zone. The domain extends for 10[m] in the y -direction (all the other measures are mentioned in Figure 3). The boundary conditions are constant injection rate on the left (bottom half of the domain pure CO₂, top half pure H₂O) and constant pressure on the right boundary (outflow) with no-flow on top and bottom.

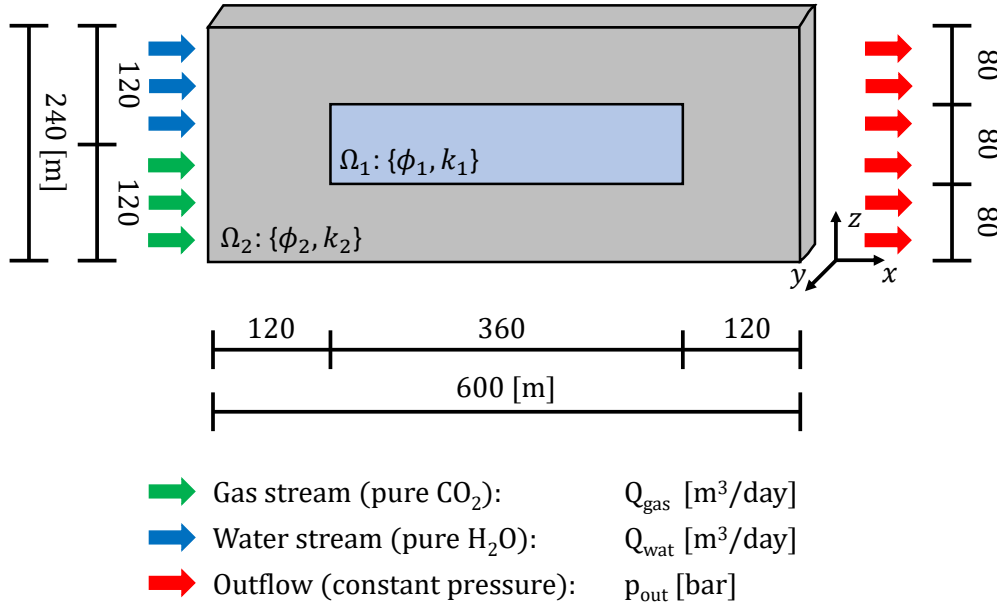


Figure 3: Configuration of the 2D test case (Section 6.2). Constant injection rate on the left boundary (Neumann) and constant pressure (Dirichlet) on the right. The domain extends 10[m] in the y -direction.

Kinetic chemistry is used to model the dissolution of CaCO₃. See Tables 5 and 6 for all the parameters

used in this model. Note that we have provided the initial values both in terms of the overall mole fractions and in terms of the individual mole fractions (computed with the same python code listed above), and also that the concentration of the calcite can be directly computed as a function of the porosity (see equation 13). All fluid and chemical parameters (e.g., kinetic constants, reference mass density, etc.) are the same as in test case 6.1.1.

In addition to the two chemical systems described later, this test case can be executed with or without gravity (i.e. $g = 0$). We note that when gravity is included, it would have been more natural for the initial pressure to follow a hydrostatic law. However, the effect is quite small, and the simpler constant initial pressure was retained.

Property	Value	Units
Gas injection rate, Q_{inj}	1000	[m ³ /day]
Water injection rate, Q_{inj}	200	[m ³ /day]
Gas injection composition, $z_{c,\text{inj}}, c = 1, \dots, C - 1$,	[0, 1, 0, 0]	[-]
Gas injection composition in molar fractions, $x_{cg,\text{inj}}, c = 1, \dots, C - 1$,	[0, 1, 0, 0]	[-]
Water injection composition, $z_{c,\text{inj}}, c = 1, \dots, C - 1$,	[1, 0, 0, 0]	[-]
Water injection composition in molar fractions, $x_{cw,\text{inj}}, c = 1, \dots, C - 1$,	[1, 0, 0, 0]	[-]
Initial pressure on $\Omega_1 \cup \Omega_2$, P_{ini}	95	[bar]
Initial composition on Ω_1 , $z_{c,\text{ini}}, c = 1, \dots, C - 1$,	[0.4, 0, 0.20, 0.20]	[-]
Initial composition on Ω_2 , $z_{c,\text{ini}}, c = 1, \dots, C - 1$,	[0.15, 0, 0.075, 0.075]	[-]
Initial fluid composition on $\Omega_1 \cup \Omega_2$ in molar fractions, $x_{cw,\text{ini}}, c = 1, \dots, C - 1$,	[0.5, 0, 0.25, 0.25]	[-]
Production pressure, P_{prod}	95	[bar]
Simulation time, T	1000	[days]

Table 5: Boundary conditions and other simulation parameters.

Property	Value	Units
Porosity on Ω_1 , ϕ	0.8	[-]
Permeability on Ω_1 , $k_{x,y,z}$	[1896, 1896, 1896]	[mD]
Porosity on Ω_2 , ϕ	0.3	[-]
Permeability on Ω_2 , $k_{x,y,z}$	[100, 100, 100]	[mD]
Total porosity on $\Omega_1 \cup \Omega_2$, ϕ^T	1	[-]
Control volume dimension, $\Delta x, y, z$	[10, 10, 10]	[m]
Number of control volumes, $N_x \times N_y \times N_z$	$60 \times 1 \times 24$	[-]
Diffusion coefficients, $d_{c_j} = d$	10^{-9}	[m ² /s]
Gravitational acceleration, g	9.8	[m/s ²]

Table 6: Values for all the relevant fluid and rock properties.

6.2.1 Simple chemical model

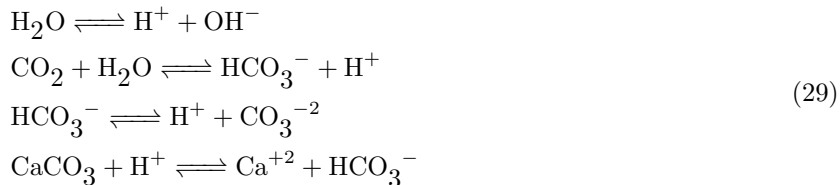
In that case, only one chemical reaction is included, and the chemical model is the same as in Section 6.1.1.

However, one further simplification may be necessary: one may encounter convergence problems when running the system as described previously. If that is the case, it may be helpful to consider a single "meta-ion" $\text{Ca}^{2+} + \text{CO}_3^{2-}$ in the liquid phase.

6.2.2 Extended chemical model

We consider a somewhat more realistic (albeit still quite small) chemical system, including dissociation of water and of carbonic dioxide, as this makes it possible to take into account the influence of pH.

The system is composed of 4 reactions:



Note that this increases the total number of species by three, particularly to $z_c = [\text{H}_2\text{O}, \text{CO}_2, \text{Ca}^{+2}, \text{CO}_3^{2-}, \text{H}^+, \text{OH}^-, \text{HCO}_3^-, \text{CaCO}_3]$. However, this allows to represent the CaCO_3 reaction (last equation in (29)) with an explicit dependency on the pH of the solution.

The first three reactions are at equilibrium, the logarithms of the equilibrium constants are given in Table 7, while the fourth reaction is kinetic, and the rate for the last reaction is given by equation (27), with Q now defined by:

$$Q = \frac{a_{\text{Ca},w} a_{\text{HCO}_3,w}}{a_{\text{H},w}}. \tag{30}$$

K_1	K_2	K_3	K_{sp}
-13.95	-6.293	-10.279	-1.899

Table 7: Log_{10} of the equilibrium constants for extended chemical system (29).

For this last case, the mass actions laws are expressed in activities:

$$\begin{aligned}
 K_1 a_{\text{H}_2\text{O},w} &= a_{\text{H}^+,w} a_{\text{OH}^-,w}, \\
 K_2 a_{\text{CO}_2,w} a_{\text{H}_2\text{O},w} &= a_{\text{HCO}_3^-,w} a_{\text{H}^+,w}, \\
 K_3 a_{\text{HCO}_3^-,w} &= a_{\text{H}^+,w} a_{\text{CO}_3^{2-},w}.
 \end{aligned} \tag{31}$$

Initial conditions computed using Arxim [Moutte et al., 2010] are given in table 8. All other physical are the same as in test 6.2.1.

7 Expected output

Participants are expected to provide the following output, in the form of a CSV file for 1D output and a figure for 2D output. To make it easier to organize the results from different participants we ask that the submitted files follow a specific naming scheme, as detailed below. Each filename name has four parts: GROUP_CASE_LOC_VAR, where

Property	Value	Units
$x_{\text{CO}_2,w}$	3.9624×10^{-10}	[-]
$x_{\text{Ca}^{2+},w}$	2.1703×10^{-6}	[-]
$x_{\text{H}^+,w}$	2.3507×10^{-12}	[-]
$x_{\text{OH}^-,w}$	1.5475×10^{-6}	[-]
$x_{\text{HCO}_3^-,w}$	1.5467×10^{-6}	[-]
$x_{\text{CO}_3^{-2},w}$	6.2315×10^{-7}	[-]

Table 8: Initial molar fractions for the extended chemical model

GROUP is a (4 to 6 character) unique identifier, selected by each group;

CASE is a 2 character identifier for the specific benchmark case, as follows

- 11 for 1D, kinetic chemistry;
- 12 for 1D, equilibrium chemistry;
- 21 for 2D, simple chemistry;
- 22 for 1D, extended chemistry.

LOC is the location of the variables in the file (such as `t1000` or `x25`);

VAR gives additional information, such as `grav` or `nograv` depending on whether or not gravity has been included.

7.1 1D homogeneous domain

- Text output of all variables as a function of space at time 1000 days in a CSV file named (with `case = "11"` or `"12"`) `GROUP_CASE_t1000.csv`, containing $(x, S_g, P_g, \phi, x_{\text{H}_2\text{O},w}, x_{\text{CO}_2,w}, x_{\text{Ca}^{2+},w} + x_{\text{HCO}_3^-,w})$;
- Text output of all variables as a function of time at $x = 25$ in a CSV file named `GROUP_CASE_x25.csv`, containing $(t, S_g, P_g, \phi, x_{\text{H}_2\text{O},w}, x_{\text{CO}_2,w}, x_{\text{Ca}^{2+},w} + x_{\text{HCO}_3^-,w})$;
- It is suggested to include a numerical convergence study.

7.2 2D heterogeneous domain

7.2.1 Simple chemical model

- Plot CO_2 fraction, ion mole fractions, gas saturation and porosity as a space maps at time 1000 days;
- Write the same variables as in 1D on a cross-section along the vertical line at $x = 40m$ in a CSV file named `GROUP_21_x40_VAR.csv`, containing $(y, S_g, P_g, \phi, x_{\text{H}_2\text{O},w}, x_{\text{CO}_2,w}, x_{\text{Ca}^{2+},w} + x_{\text{HCO}_3^-,w})$;
- Write the same variables as in 1D on a cross-section along the horizontal line at $y = 50m$ in a CSV file named `GROUP_21_y50_VAR.csv`, containing $(x, S_g, P_g, \phi, x_{\text{H}_2\text{O},w}, x_{\text{CO}_2,w}, x_{\text{Ca}^{2+},w} + x_{\text{HCO}_3^-,w})$.

7.2.2 Extended chemical model

Same output as for the simple chemical model, with the addition of all chemical species:

- Plot CO₂ fraction, ion mole fractions, gas saturation and porosity as a space maps at time 1000 days;
- Text output of the same variables as 1D cross-section along vertical line at $x = 40m$ in a CSV file named GROUP_22_x40.csv, containing $(y, S_g, P_g, x_{H_2O,w}, x_{CO_2,w}, x_{Ca^{2+},w}, x_{H^+,w}, x_{HCO_3^-,w}, x_{CO_3^{2-},w}, \phi)$;
- Write the same variables as in 1D on a cross-section along the horizontal line at $(y = 50m$ in a CSV file named GROUP_22_y50.csv, containing $(y, S_g, P_g, x_{H_2O,w}, x_{CO_2,w}, x_{Ca^{2+},w}, x_{H^+,w}, x_{HCO_3^-,w}, x_{CO_3^{2-},w}, \phi)$.

Acknowledgements

The authors are grateful to Eric Flauraud (IFPEN) for providing the initial values for the "Extended chemical model" in Section 6.2.2, as well as for a careful reading of the paper.

A Appendix

1D injection

Properties based on injection state: state = [P, z_h2o, z_co2, z_ca, z_co3]

Injection state = [1.65e+02 1.00e-12 1.00e+00 1.00e-12 1.00e-12]

```
-----
                H2O          CO2          Ca+2          CO3-2          CaCO3
Composition, z_c 1.00e-12    1.00e+00    1.00e-12    1.00e-12    1.00e-12
Liquid MoleFrac  1.00e-11    1.00e-02    4.94e-01    4.94e-01    0.00e+00
Vapor MoleFrac   1.00e-12    1.00e+00    4.94e-13    4.94e-13    0.00e+00
Solid MoleFrac   0.00e+00    0.00e+00    0.00e+00    0.00e+00    1.00e+00
-----
```

```
-----
                Liquid      Vapor      Solid
Phase MoleFrac  1.02e-12    1.00e+00    1.00e-12
Mass Density    1.00e+03    1.01e+02    2.00e+03
Viscosity       1.00e+00    1.00e-01    0.00e+00
Sat. phi_tot    1.17e-13    1.00e+00    1.00e-12
Sat. phi_fluid  1.17e-13    1.00e+00    0.00e+00
-----
```

1D initial

Properties based on initial state: state = [P, z_h2o, z_co2, z_ca, z_co3]

Initial state = [9.5e+01 1.5e-01 1.0e-12 7.5e-02 7.5e-02]

```
-----
                H2O          CO2          Ca+2          CO3-2          CaCO3
Composition, z_c 1.50e-01    1.00e-12    7.50e-02    7.50e-02    7.00e-01
-----
```

Liquid MoleFrac	5.00e-01	3.33e-12	2.50e-01	2.50e-01	0.00e+00
Vapor MoleFrac	5.00e-01	3.33e-12	2.50e-01	2.50e-01	0.00e+00
Solid MoleFrac	0.00e+00	0.00e+00	0.00e+00	0.00e+00	1.00e+00

	Liquid	Vapor	Solid
Phase MoleFrac	3.00e-01	0.00e+00	7.00e-01
Mass Density	1.00e+03	1.00e+02	2.00e+03
Viscosity	1.00e+00	1.00e-01	0.00e+00
Sat. phi_tot	3.00e-01	0.00e+00	7.00e-01
Sat. phi_fluid	1.00e+00	0.00e+00	0.00e+00

2D initial (rock, Ω_2)

Properties based on initial state: state = [P, z_CO2, z_Ions, z_H2O]

initial state = [9.5e+01 1.0e-12 1.5e-01 1.5e-01]

	CO2	Ions	H2O	CaCO3
Composition, z_c	1.0000000e-12	1.5000000e-01	1.5000000e-01	7.0000000e-01
Vapor MoleFrac	9.5454581e-01	4.5000000e-13	4.5454545e-02	0.0000000e+00
Liquid MoleFrac	3.3333333e-12	5.0000000e-01	5.0000000e-01	0.0000000e+00
Solid MoleFrac	0.0000000e+00	0.0000000e+00	0.0000000e+00	1.0000000e+00

	Vapor	Liquid	Solid
Phase MoleFrac	0.0000000e+00	3.0000000e-01	7.0000000e-01
Mass Density	1.0094000e+02	1.0000940e+03	2.0000000e+03
Viscosity	1.0000000e-01	1.0000000e+00	0.0000000e+00
Sat. phi_tot	0.0000000e+00	3.0000000e-01	7.0000000e-01
Sat. phi_fluid	0.0000000e+00	1.0000000e+00	0.0000000e+00

2D initial (void, Ω_1)

Properties based on initial state: state = [P, z_CO2, z_Ions, z_H2O]

initial state = [9.50000000e+01 2.66666667e-12 4.00000000e-01 4.00000000e-01]

	CO2	Ions	H2O	CaCO3
Composition, z_c	2.6666667e-12	4.0000000e-01	4.0000000e-01	2.0000000e-01
Vapor MoleFrac	9.5454581e-01	4.5000000e-13	4.5454545e-02	0.0000000e+00
Liquid MoleFrac	3.3333333e-12	5.0000000e-01	5.0000000e-01	0.0000000e+00
Solid MoleFrac	0.0000000e+00	0.0000000e+00	0.0000000e+00	1.0000000e+00

	Vapor	Liquid	Solid
--	-------	--------	-------

Phase MoleFrac	0.0000000e+00	8.0000000e-01	2.0000000e-01
Mass Density	1.0094000e+02	1.0000940e+03	2.0000000e+03
Viscosity	1.0000000e-01	1.0000000e+00	0.0000000e+00
Sat. phi_tot	0.0000000e+00	8.0000000e-01	2.0000000e-01
Sat. phi_fluid	0.0000000e+00	1.0000000e+00	0.0000000e+00

2D injection (water stream)

Properties based on injection state: state = [P, z_CO2, z_Ions, z_H2O]
injection state = [9.5e+01 2.0e-12 1.0e-12 1.0e+00]

	CO2	Ions	H2O	CaCO3
Composition, z_c	2.0000000e-12	1.0000000e-12	1.0000000e+00	9.9997788e-13
Vapor MoleFrac	9.0909267e-01	9.0000000e-25	9.0909091e-02	0.0000000e+00
Liquid MoleFrac	2.0000000e-12	1.0000000e-12	1.0000000e+00	0.0000000e+00
Solid MoleFrac	0.0000000e+00	0.0000000e+00	0.0000000e+00	1.0000000e+00

	Vapor	Liquid	Solid
Phase MoleFrac	0.0000000e+00	1.0000000e+00	9.9997788e-13
Mass Density	1.0094000e+02	1.0000940e+03	2.0000000e+03
Viscosity	1.0000000e-01	1.0000000e+00	0.0000000e+00
Sat. phi_tot	0.0000000e+00	1.0000000e+00	9.9997788e-13
Sat. phi_fluid	0.0000000e+00	1.0000000e+00	0.0000000e+00

2D injection (gas stream)

Properties based on injection state: state = [P, z_CO2, z_Ions, z_H2O]
injection state = [9.5000000e+01 1.0000000e+00 1.0000000e-12 9.9997788e-13]

	CO2	Ions	H2O	CaCO3
Composition, z_c	1.0000000e+00	1.0000000e-12	9.9997788e-13	9.9997788e-13
Vapor MoleFrac	1.0000000e+00	9.0008986e-13	9.9997788e-13	0.0000000e+00
Liquid MoleFrac	1.0000000e-01	9.0008986e-01	9.9997788e-12	0.0000000e+00
Solid MoleFrac	0.0000000e+00	0.0000000e+00	0.0000000e+00	1.0000000e+00

	Vapor	Liquid	Solid
Phase MoleFrac	1.0000000e+00	1.2478907e-13	9.9997788e-13
Mass Density	1.0094000e+02	1.0000940e+03	2.0000000e+03
Viscosity	1.0000000e-01	1.0000000e+00	0.0000000e+00
Sat. phi_tot	1.0000000e+00	1.4150213e-14	9.9997788e-13
Sat. phi_fluid	1.0000000e+00	1.4150213e-14	0.0000000e+00

References

- [Farshidi, 2016] Farshidi, S. F. (2016). *Compositional reservoir simulation-based reactive-transport formulations, with application to CO₂ storage in sandstone and ultramafic formations*. PhD thesis, Stanford University.
- [Kala and Voskov, 2020] Kala, K. and Voskov, D. (2020). Element balance formulation in reactive compositional flow and transport with parameterization technique. *Computational Geosciences*, 24(2):609–624.
- [Moutte et al., 2010] Moutte, J., Michel, A., Battaia, G., Parra, T., Garcia, D., and Wolf, S. (2010). Arxim, a library for thermodynamic modeling of reactive heterogeneous systems, with applications to the simulation of fluid-rock system. In *21st Congress of IUPAC*. Conference on Chemical Thermodynamic, Tsukuba, Japan.